Langmuir

Article

pubs.acs.org/Langmuir

Preparation and Characterization of Reconstituted Lipid−Synthetic Polymer Discoidal Particles

Masafumi Tanaka,*[,†] Akira Hosotani,[†] Yuka Tachibana,[†] Minoru Nakano,[‡] Kenji Iwasaki,[§] Toru Kawakami,[∥] and Takahiro Mukai[†]

[†]Department of Biophysical Chemistry, Kobe Pharmaceutical University, Kobe 658-8558, Japan

[‡]Graduate School of Medicine and Pharmaceutical Sciences, University of Toyama, Toyama 930-0194, Japan

[§]Laboratory of Protein Synthesis and Expression, Institute for Protein Research, and [∥]Laboratory of Protein Organic Chemistry, Institute for Protein Research, Osaka University, Suita 565-0871, Japan

ABSTRACT: Discoidal high-density lipoproteins generated by the apolipoprotein-mediated solubilization of membrane lipids *in vivo* can be reconstituted with phospholipids and apolipoproteins *in vitro*. Recently, it has been reported that such particles can be prepared using the hydrolyzed acid form of styrene−maleic anhydride copolymer (SMAaf) instead of apolipoproteins, but characterization of its physicochemical properties has remained less elucidated. In the present study, with the aim of applying SMAaf-based lipid nanoparticles as novel delivery vehicles of drugs and/or imaging agents, we investigated the preparation conditions and evaluated the physicochemical properties of lipid−SMAaf complexes. SMAaf induced spontaneous turbidity clearance of dimyristoylphosphatidylcholine (DMPC) vesicles accompanied by the formation of smaller particles not only at the phase transition temperature of DMPC but also above it. Such reductions in the turbidity were not observed with some other amphiphilic synthetic polymers tested under the same experimental conditions. Size exclusion chromatography analyses showed that homogeneously sized particles were prepared at lipid to SMAaf weight ratios of less than 1/1.5. Dynamic light scattering and transmission electron microscopy revealed that gel-filtered DMPC−SMAaf complexes were approximately 8−10 nm in diameter and discoidal in shape. The DMPC−SMAaf complexes were relatively stable even after lyophilization but were sensitive to pH changes. Fluorescence techniques demonstrated that the gel to liquid-crystalline phase transition temperature of DMPC in the discoidal complexes broadened significantly relative to that of liposomes, despite their common bilayer structure, which is a typical feature of discoidal lipid nanoparticles. These results provide fundamental insights into discoidal SMAaf-based lipid nanoparticles for the development of novel delivery vehicles.

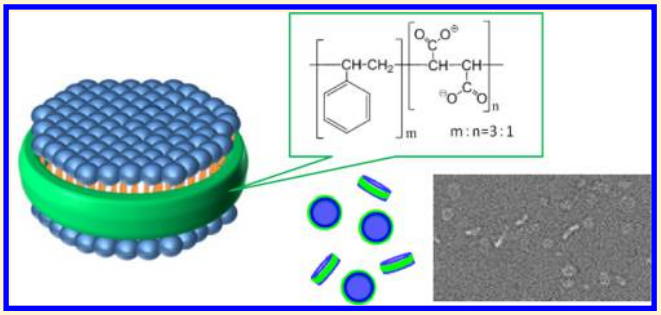

1. INTRODUCTION

Plasma high-density lipoproteins (HDLs) are lipid−protein complexes of nanometer sizes crucial for the transportation of lipids in the blood circulation. In plasma, HDLs may exist as either spherical or discoidal particles.[1] Spherical HDL contains a core of neutral lipids, such as triglycerides or cholesteryl esters, surrounded mainly by phospholipid and cholesterol monolayer and apolipoproteins. Discoidal HDL is predominantly composed of phospholipid bilayer disc whose periphery is circumscribed by apolipoprotein molecules. At the very beginning of HDL generation, discoidal particles are formed, after which they acquire neutral lipids and mature into spherical particles. The most abundant apolipoprotein component of plasma HDL is apolipoprotein A-I (apoA-I), which possesses a series of amphipathic helical motifs in the amino acid sequence.[2] Discoidal HDL particles can be reconstituted with phospholipids and apolipoproteins or even their analogues.[3,4]

Although discoidal HDL particles are structurally similar to well-characterized model liposome membrane in terms of bearing phospholipid bilayer, unique physicochemical and biological properties of discoidal nanoparticles allow their use in various nanobiotechnology applications. In particular, discoidal nanoparticles, termed Nanodiscs, consisting of membrane scaffold protein (MSP) are widely used for studies of membrane proteins.[5] Because MSP has been designed on the basis of the human apoA-I sequence, Nanodiscs are essentially identical to nascent HDL. In addition, the apoA-I mimetic peptide has been shown to form discoidal particles that can stabilize membrane proteins.[6] Moreover, discoidal nanoparticles offer an ideal environment as a platform for poorly water-soluble drugs. For example, the incorporation of amphotericin B or curcumin into discoidal nanoparticles has been shown to improve the solubility of these substances and thereby enhance the efficacy of the drugs.[7,8] Taken together with the fact that HDL is a natural carrier of lipophilic compounds in plasma, the application of discoidal nanoparticles

Received: September 13, 2015
Revised: October 30, 2015
Published: November 4, 2015

DOI: 10.1021/acs.langmuir.5b03438
Langmuir 2015, 31, 12719−12726

is not limited only to their use as membrane mimics in the realm of structural biology, but they can also be used as transport/delivery vehicles of drugs.[9]

Initially, we sought to make use of discoidal HDL composed of apolipoproteins or their mimetic peptides for bioimaging applications. However, there are some limitations for clinical application of such discoidal nanoparticles, particularly in terms of productivity because proteins or peptides are expensive, and regarding the safety because apolipoproteins are usually obtained from plasma or *Escherichia coli*. Recently, it has been revealed that a synthetic polymer, styrene–maleic acid, forms discoidal nanoparticles similar to those of reconstituted HDL (rHDL).[10] HDL-mimicking lipid particles composed of styrene–maleic acid instead of apolipoproteins are referred to as SMALPs and are commercially available as Lipodisq. Styrene–maleic acid polymer is biocompatible; consequently, its lipid complexes can be used clinically.[11,12] Nevertheless, the detailed structural characterization of lipid–synthetic polymer complexes is highly limited. In the present study, the preparation conditions and physicochemical properties of lipid–synthetic polymer complexes were investigated with the goal of contributing to the future development of delivery vehicles.

2. EXPERIMENTAL PROCEDURES

2.1. Materials. 1,2-Dimyristoyl-*sn*-glycero-3-phosphocholine (DMPC) and 1-palmitoyl-2-oleoyl-*sn*-glycero-3-phosphocholine (POPC) were purchased from NOF Corporation (Tokyo, Japan). Prehydrolyzed styrene–maleic anhydride copolymer 3:1 (SMAaf; molecular weight, $M_w \sim 9500$) and poly(methacrylic acid) ($M_w \sim 7750$) were purchased from Sigma-Aldrich (St. Louis, MO). Polyvinylpyrrolidone ($M_w \sim 46\,600$) was purchased from Wako Pure Chemicals (Osaka, Japan). Pluronic F-127 was purchased from Anatrace (Maumee, OH). 6-Dodecanoyl-2-dimethylaminonaphthalene (Laurdan) was purchased from AnaSpec (Fremont, CA). Lissamine Rhodamine B 1,2-dihexadecanoyl-*sn*-glycero-3-phosphoethanolamine (Rhodamine-PE) and 1,2-bis(1-pyrenebutanoyl)-*sn*-glycero-3-phosphocholine (dipy-PC) were obtained from Molecular Probes (Eugene, OR).

Because the term "SMA" is generally used for its anhydride form, the hydrolyzed acid form is referred to as SMAaf in this paper to differentiate the two. The extinction coefficient of SMAaf was determined for quantification using a Shimadzu UV-2450 spectrophotometer (Kyoto, Japan). The absorbance at 268 nm, which is derived from the aromatic ring of styrene,[13] increased in a concentration-dependent manner (Figure 1). The large amount of absorption near 225 nm is probably derived from maleic acid.[14] The calculated value for the extinction coefficient of SMAaf in 1.0 M NaOH was 0.866 (mL mg^{-1} cm^{-1}). Concentrations of other polymers with no characteristic absorbance were determined by actual weight value. No fluorescence derived from SMAaf was detected under our experimental conditions mentioned below.

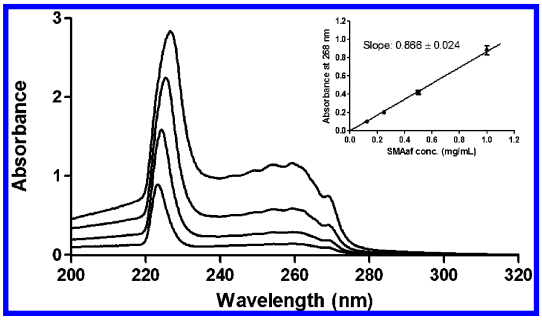

Figure 1. Absorption spectra of SMAaf in 1.0 M NaOH. The concentrations used were 1.0, 0.5, 0.25, and 0.125 mg/mL in descending order. (inset) Linear relationship between the SMAaf concentration and the absorbance at 268 nm. Plots are represented as the mean ± SEM (N = 12).

2.2. Phospholipid Solubilization Assay. Phospholipids were dried under vacuum, dispersed in 10 mM sodium phosphate buffer (pH 7.4) with vigorous vortex mixing, and subjected to five freeze–thaw cycles. The kinetics of phospholipid vesicle solubilization after the addition of synthetic polymers were monitored by right-angle light scattering performed on a Hitachi F-2500 spectrophotometer (Tokyo, Japan), as previously described.[15] Excitation and emission wavelengths were set at 600 nm. Phospholipid vesicles (final concentrations of 50 μg/mL) were incubated at a lipid to synthetic polymer weight ratio of 1/2, unless otherwise noted, for 10 min at 15, 25, or 35 °C. The presence of trace amount of fluorescent probes did not affect the solubilization of phospholipid vesicles. Phospholipid concentrations were determined using a colorimetric enzymatic assay kit for choline (Wako Pure Chemicals).

2.3. Size Exclusion Chromatography (SEC). Lipid–SMAaf complexes were prepared by the self-assembly method at 25 °C overnight in a manner similar to that used for the phospholipid solubilization assay. Isolation of lipid–SMAaf complexes from larger particles and free SMAaf was performed on a Superdex 200 prep grade XK 16/600 column (GE Healthcare, Buckinghamshire, UK) at a flow rate of 1.0 mL/min controlled by a Biologic FPLC (Bio-Rad, Hercules, CA). Ultraviolet (UV) absorbance at 280 nm, presumably attributable to the light scattering, was monitored. Fluorescence of a trace amount (1.0 mol %) of Rhodamine-PE incorporated into phospholipid was concomitantly measured.

2.4. Dynamic Light Scattering (DLS). Size distributions of the lipid–SMAaf complexes were determined by using DLS measurements at 25 °C performed on a Zetasizer Nano ZS (Malvern, Worcestershire, UK) equipped with a He–Ne laser as a light source. Data were collected for 50–70 s and averaged for three scans. The number-average diameters were obtained by assuming that the particles were spherical and undergoing Brownian motion.

2.5. Transmission Electron Microscopy (TEM). A carbon-coated copper grid (400 mesh) was subjected to hydrophilic treatment. Freshly prepared lipid–SMAaf complexes were adsorbed onto the grid and negatively stained with 2% (w/v) ammonium molybdate (adjusted to neutral pH). The grid was examined using a JEM-2200FS transmission electron microscope (JEOL, Tokyo, Japan) operated at 200 kV. Zero energy-loss images obtained using an in-column filter (omega filter) with a slit width of 14 eV were recorded on a K2 summit direct electron detection camera (Gatan, Inc., Pleasanton, CA) operated in counting mode. A dose fractionation mode and the motion-correction technique were utilized to compensate for specimen motion.[16] Each single exposure image was composed of 25 subframes recorded every 0.2 s.

2.6. Stability Test. The stabilities of lipid–SMAaf complexes kept at 4 or 37 °C were evaluated for a period of 7 days at a phospholipid concentration of 100 μg/mL. To assess the stabilities against lyophilization, 800 μL of lipid–SMAaf complexes was freeze-dried in a Model FDU-1200 chamber (EYELA, Tokyo, Japan). The samples were frozen, dried under vacuum, and rehydrated to their original volume with ultrapure water. To assess the stabilities against pH changes, 950 μL of lipid–SMAaf complexes in 10 mM sodium phosphate buffer (pH 7.4) was mixed with 50 μL of dilute phosphoric acid. The final pH values of the solutions were measured using a standardized pH meter.

2.7. Generalized Polarization (GP) Measurements. GP measurements of Laurdan were performed at an excitation wavelength of 340 nm, and the spectra were recorded from 400 to 600 nm at every 5 °C interval from 5 to 40 °C on a Hitachi F-7000 spectrophotometer. Laurdan was added to lipid particles prior to the evaporation at a probe to phospholipid molar ratio of 1/200. Samples were diluted to 10–30 μM phospholipid concentration and constantly stirred during measurements. GP values were obtained by calculating the dual-wavelength ratio of the emission intensities at 440 nm (I_{440}) and 490 nm (I_{490}).[17]

DOI: 10.1021/acs.langmuir.5b03438
Langmuir 2015, 31, 12719–12726

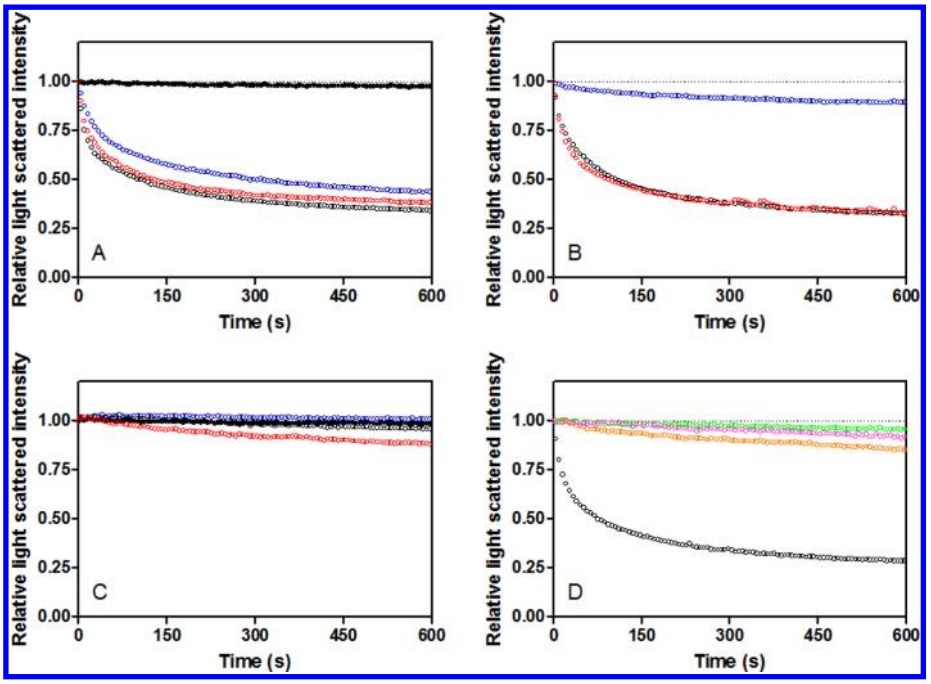

Figure 2. (A) DMPC vesicle solubilization by SMAaf at different ratios at 25 °C (blue for 1/1, black for 1/2, red for 1/3, and closed for no SMAaf). (B) DMPC vesicle solubilization by SMAaf at various temperatures (blue for 15 °C, black for 25 °C, red for 35 °C). (C) POPC vesicle solubilization by SMAaf at various temperatures (blue for 15 °C, black for 25 °C, red for 35 °C, and closed for no SMAaf at 25 °C). (D) DMPC vesicle solubilization by other polymers at 25 °C (black for SMAaf, green for poly(methacrylic acid), pink for polyvinylpyrrolidone, and orange for Pluronic F-127).

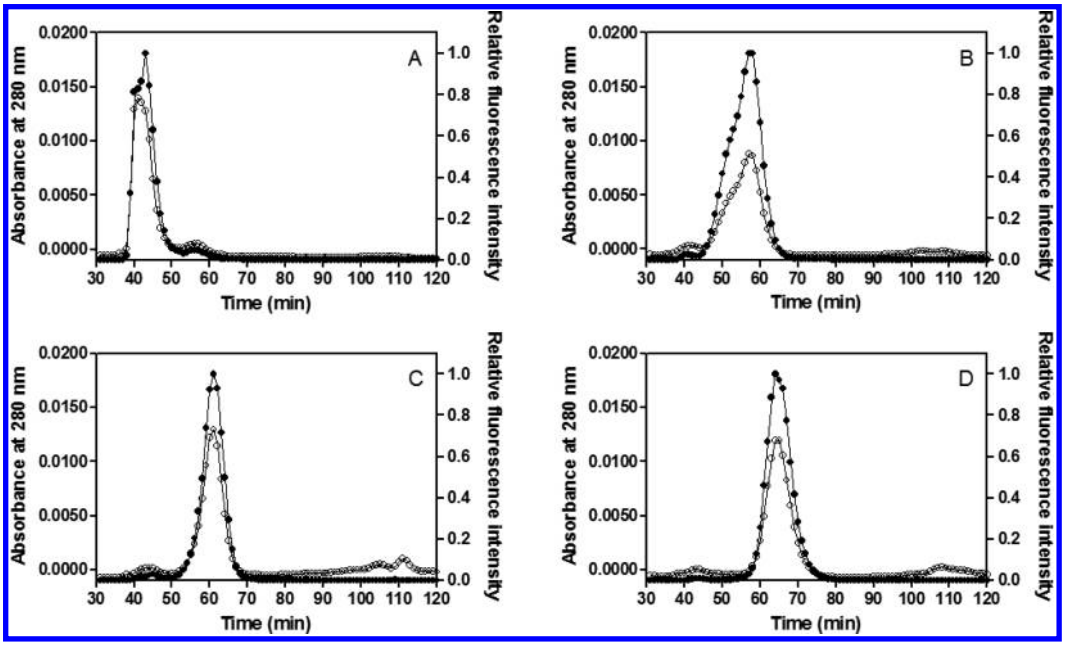

Figure 3. SEC profiles of DMPC−SMAaf complexes monitored by UV absorbance at 280 nm (dashed line) and Rhodamine fluorescence (solid line). The DMPC to SMAaf weight ratios were (A) 1/0.5, (B) 1/1, (C) 1/1.5, and (D) 1/2.

2.8. Pyrene Excimer Formation Measurements. Pyrene excimer formation experiments were performed using an excitation wavelength of 342 nm, and the spectra were recorded from 350 to 600 nm at every 5 °C interval from 5 to 40 °C on a Hitachi F-7000 spectrophotometer. Pyrene-labeled lipid particles containing 0.1 mol % dipy-PC were diluted to 10 μM phospholipid concentrations and constantly stirred during measurements. The emission intensities at 377 nm (monomer, I_m) and 479 nm (excimer, I_e) were chosen to determine the excimer to monomer fluorescence intensity ratio (I_e/I_m).

3. RESULTS

3.1. Solubilization of Phospholipid Vesicles by SMAaf. Spontaneous lipid solubilization caused by apolipoproteins has been widely examined by determining the time-dependent decrease in light scattering intensity due to the formation of rHDL.[18] The typical time courses of lipid solubilization by synthetic polymers are shown in Figure 2. In the absence of any polymers, the light scattering intensity derived from the lipid vesicles was almost unchanged at any temperatures tested. At

DOI: 10.1021/acs.langmuir.5b03438
Langmuir 2015, 31, 12719−12726

25 °C, the addition of SMAaf caused the solubilization of DMPC vesicles in a manner similar to apolipoproteins (Figure 2A). The dependences of the lipid to SMAaf weight ratios were initially examined at 25 °C (Figure 2A). The time courses at DMPC to SMAaf weight ratios of 1/2 and 1/3 were nearly identical, although that of 1/1 was slightly slower. To ascertain the importance of the gel to liquid-crystalline phase transition temperature (T_m), DMPC solubilization was further examined at 15 and 35 °C (Figure 2B). Unlike apolipoproteins, solubilization of DMPC vesicles also occurred at temperatures much above the T_m (35 °C), but not below it (15 °C). These results prompted us to investigate whether such spontaneous lipid solubilization occurs with POPC, of which the T_m is below 0 °C. Unexpectedly, no apparent changes in the light scattering intensity of POPC vesicles were observed by the addition of SMAaf at any temperature tested (Figure 2C). In the presence of other amphiphilic polymers, such as poly(methacrylic acid), polyvinylpyrrolidone, or Pluronic F-127, no significant changes in the light scattering intensity of DMPC vesicles were observed at 25 °C (Figure 2D), which suggested that lipid solubilization is highly dependent on polymer structure.

3.2. Preparation Conditions of DMPC−SMAaf Complexes. Comparison of the SEC profiles of lipid−synthetic polymer complexes provides insight into particle sizes and homogeneity. Although the absorption intensity of SMAaf at 280 nm is extremely weak, small peaks derived from free SMAaf appeared near 110 min (data not shown). Given the average M_w, free SMAaf should have eluted as a monomer. When complex formation was performed at a lipid to SMAaf weight ratio of 1/0.5, the main peak appeared near 40 min (Figure 3A), which showed larger particle sizes of approximately 30−100 nm in diameter. This peak was assumed to be derived from SMAaf-free unincorporated or SMAaf-poor lipid particles because of a lack of SMAaf available for complex formation. On the other hand, at a lipid to SMAaf weight ratio of 1/1, the peak derived from DMPC−SMAaf complexes appeared at approximately 60 min (Figure 3B) with a relatively broad shoulder on the left side of the peak. Although a peak near 110 min was apparently observed, it disappeared when monitored by Rhodamine-PE fluorescence, which showed that these fractions contained no lipids. At lipid to SMAaf weight ratios of 1/1.5 and 1/2, the peak patterns were similar and the peak positions were almost identical (Figures 3C,D). The SEC profiles were highly reproducible. Further characterizations were performed using DMPC−SMAaf complexes prepared at a lipid to SMAaf weight ratio of 1/2.

3.3. Characterization of DMPC−SMAaf Complexes. Fractions surrounding the peak were collected and further analyzed. DLS measurements revealed that the DMPC−SMAaf complexes were monodispersed, and the particle diameters were approximately 8−10 nm, which corresponds to the size of native HDL (Figure 4A). To ascertain whether these nanosized complexes were discoidal, the morphologies of the complexes were visualized using TEM. Similar to the images of rHDL particles composed of apolipoproteins, the TEM showed typical patterns of circular and rectangular mixtures (Figure 4B). These images corresponded to the top and side views of the particles, suggesting that the overall shape is discoidal. Discoidal morphology of DMPC−SMAaf complexes has been assumed on the basis of spin-label electron paramagnetic resonance spectroscopy findings.[10] Of note, many circular assemblies have appeared to have a toroidal shape, possibly because of enhanced electron density on the edge of the discoidal particles. No evidence of rouleaux formation by the stacking of discoidal particles, which is an artifact of using phosphotungstic acid for negative staining,[19] were found. Uranyl staining, which is usually performed in TEM observations for rHDL particles, was avoided because the DMPC−SMAaf complexes are highly sensitive to the solution pH, as described below.

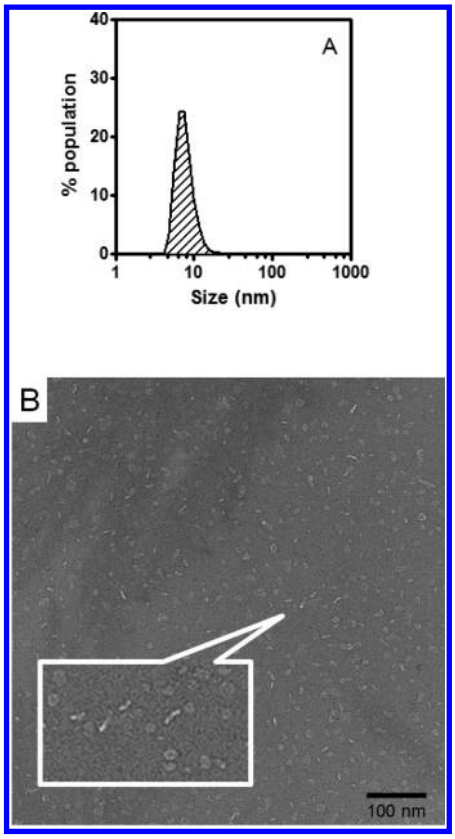

Figure 4. (A) Size distributions of DMPC−SMAaf complexes at 25 °C. (B) TEM image of DMPC−SMAaf complexes.

3.4. Stability of DMPC−SMAaf Complexes. The colloidal stability of the DMPC−SMAaf complexes stored under nitrogen either at 4 or 37 °C was assessed by DLS. At both temperatures, no significant changes in the particle distributions were observed over a period of at least 7 days (Figures 5A,B), which indicated that the DMPC−SMAaf complexes remained stable. From an experimental point of view, these results were advantageous because we did not need to expend freshly prepared particles in haste. Freeze-drying is a more promising way of obtaining pharmaceutically useful formulations with a long shelf life. Thus, the changes in particle diameters upon freeze-drying of DMPC−SMAaf complexes were also evaluated. Figure 5C compares the size distributions of the DMPC−SMAaf complexes before dehydration and after rehydration. Although marked increases in the size distributions occurred only occasionally, the distribution pattern tended to shift to slightly larger sizes with freeze-drying in most cases, as shown in Figure 5C, suggesting that the DMPC−SMAaf complexes were fairly stable against freeze-drying. Because we unexpectedly found that acidification caused a marked increase in turbidity, the stability of DMPC−SMAaf complexes against pH changes was tested (Figure 5D). Solutions of DMPC−SMAaf complexes were rendered acidic by adding dilute phosphoric acid to solutions prepared at pH 7.4. When the

DOI: 10.1021/acs.langmuir.5b03438
Langmuir 2015, 31, 12719−12726

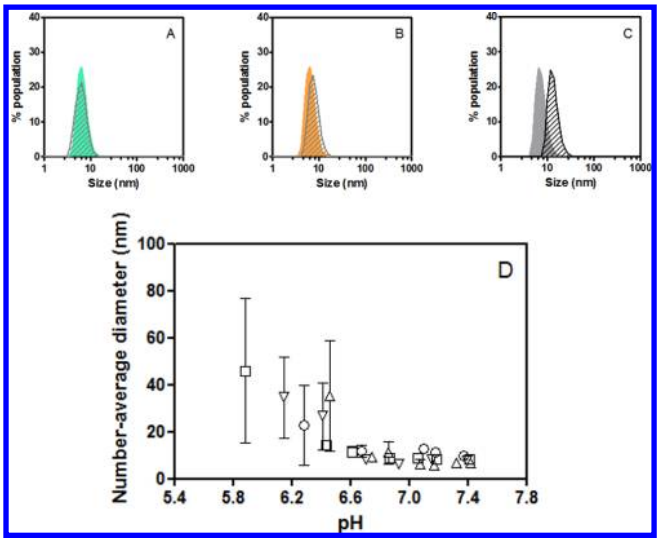

Figure 5. Changes in the size distributions of DMPC−SMAaf complexes stored at (A) 4 °C or (B) 37 °C. Slashed peak: after storage. (C) Effect of lyophilization on the size distributions of DMPC−SMAaf complexes. Slashed peak: after lyophilization. (D) Effect of solution pH changes on the number-average diameters of DMPC−SMAaf complexes.

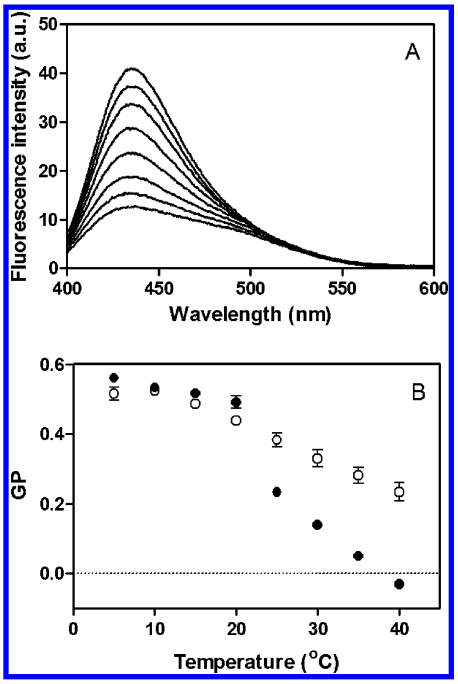

Figure 6. (A) Representative Laurdan emission spectra in DMPC−SMAaf complexes at an excitation wavelength of 340 nm from 5 to 40 °C in ascending order of temperature beginning at the top. (B) GP values of Laurdan measured in DMPC vesicles (closed circles) and DMPC−SMAaf complexes (open circles) as a function of temperature.

solution pH reached below 6.6, which is roughly corresponding to the pK_a (where K_a is the acid dissociation constant) of maleic acid, a prominent secondary peak was observed so that the average diameters became noticeably larger, which suggested that the DMPC−SMAaf complexes were sensitive to solution pH.

3.5. GP Measurements. To gain information about the membrane properties of the DMPC−SMAaf complexes, Laurdan fluorescence, which is sensitive to the polarity and dynamics of the environment, was used.[20] In DMPC vesicles, the emission spectrum of Laurdan was red-shifted upon heating, which reflected the transition from the gel to liquid-crystalline phase (data not shown). Specifically, at 5−20 °C, the emission spectrum of the DMPC vesicles was dominated by an emission maximum at 440 nm, which indicated the existence of the gel phase. As the temperature increased above 25 °C, the emission maximum became centered at a wavelength of about 490 nm. In contrast, gradual decreases in the emission maximum at 440 nm of the DMPC−SMAaf complexes were observed upon heating, which was similar to the case observed for the DMPC vesicles, but no apparent emergence of the emission maximum with 490 nm occurred (Figure 6A). The temperature dependence of the Laurdan GP values was monitored (Figure 6B). In the DMPC vesicles, the typical behavior of Laurdan GP was observed with an abrupt decrease at the transition temperature near 25 °C. On the other hand, a modest decrease of Laurdan GP was observed in the DMPC−SMAaf complexes, which was markedly more gradual than that observed in MSP Nanodiscs.[21] These results were consistent with the differential scanning calorimetry results showing that lipids incorporated into the DMPC−SMAaf complexes did not undergo a highly cooperative phase transition and had a broader phase transition than the MSP Nanodiscs did.[10]

3.6. Pyrene Excimer Formation Measurements. Pyrene shows two typical components of the emission spectra derived from excited monomers at shorter wavelengths and dimers (excimers) at longer wavelengths. Excimers are formed when a molecule in the excited state collides with a molecule in the ground state.[22] Formation of intramolecular excimers is a characteristic feature of dipy-PC molecules. An increase in membrane fluidity enhances the collision frequency between pyrene moieties, which thereby increases the I_e/I_m value. Thus, dipy-PC detects the changes in the membrane dynamics accompanied by the transition from the gel to liquid-crystalline phase from a different aspect. The concentrations of dipy-PC were set to 0.1 mol % to minimize the effect of intermolecular excimer formation. The emission spectra of dipy-PC in the DMPC−SMAaf complexes are shown in Figure 7A. Only slight excimer fluorescence was observed at 5 °C, but the broad, red-shifted peak around 480 nm was enlarged at 40 °C, relative to the sharp peak at 377 nm. Figure 7B shows the temperature dependences of the I_e/I_m values of the DMPC vesicles and DMPC−SMAaf complexes. The I_e/I_m values of the DMPC vesicles increased abruptly near the transition temperature, whereas those in the DMPC−SMAaf complexes broadened or eliminated the transition in a manner similar to the Laurdan GP measurements. Decreased membrane fluidity in the DMPC−SMAaf complexes at higher temperatures was attributed to the existence of boundary lipids remaining in a more ordered state, as is the case with rHDL particles composed of apolipoproteins. However, such highly rigid membrane properties of DMPC−SMAaf complexes even at physiological temperature may be a unique characteristic never observed in MSP Nanodiscs.[21]

4. DISCUSSION

4.1. Preparation Conditions for Lipid−SMAaf Complexes. Regarding liposomes as delivery vehicles, POPC is one of the most widely used phospholipid components.[23] Under our preparation conditions, SMAaf did not solubilize POPC vesicles. It has been reported that lipid−SMAaf complexes can be prepared from vesicles composed of POPC containing 10 mol % phosphatidylglycerol (PG).[24] PG is a negatively charged

DOI: 10.1021/acs.langmuir.5b03438
Langmuir 2015, 31, 12719−12726

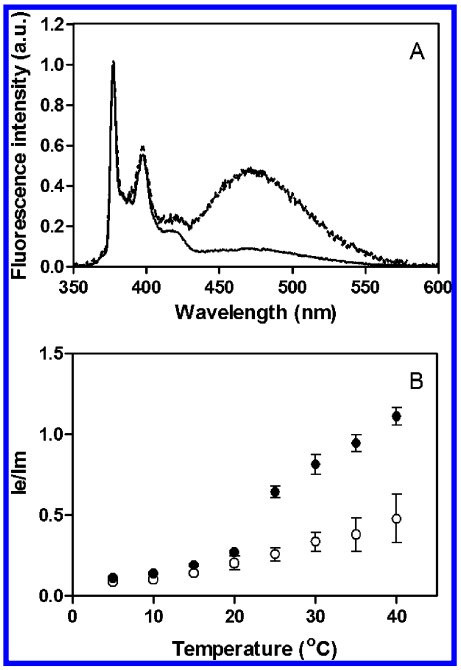

Figure 7. (A) Representative dipy-PC emission spectra in DMPC–SMAaf complexes at an excitation wavelength of 342 nm at 5 °C (solid line) and 40 °C (dashed line). (B) I_e/I_m values of dipy-PC measured in DMPC vesicles (closed circles) and DMPC–SMAaf complexes (open circles) as a function of temperature.

phospholipid often used to enhance the efficiency of rHDL formation by apolipoproteins.[25] Alternatively, freeze/sonication cycles might have improved the efficiency of lipid–SMAaf complex formation. The previous finding that lipid to polymer weight ratios of smaller than 1/1.25 were required for complete solubilization of POPC/PG vesicles[24] was consistent with the present observation that homogeneously sized particles could be prepared at a lipid to SMAaf weight ratio of less than 1/1.5, although the size of the nanoparticles was much larger (radius: 30 nm) than that of the DMPC–SMAaf complexes in our study.

Another recent study showed that SMAaf is a highly efficient membrane-solubilizing agent and does not preferentially solubilize specific lipid species.[26] The possible reasons for such discrepancies across studies are uncertain, but the most critical differences might be the SMA polymer used (a styrene to maleic acid ratio of 2/1 vs 3/1), as discussed below. It is also likely that the differences in the pH of the buffer (pH 8.0 vs 7.4) affect the solubilizing ability, but our preliminary observations showed no effective clearance of POPC vesicles, even at pH 8.0. Differences in the lamellarity and size of vesicles might affect the efficiency of solubilization. Thus, we cannot completely rule out the possibility that lipid–SMAaf complexes are formed with POPC by SMAaf-induced spontaneous lipid solubilization. Although another standard method for preparing rHDL, a cholate dialysis method, may enable the creation of POPC–SMAaf complexes, it would be unfavorable from a practical application perspective.

4.2. Structural Requirement of Polymers for Complex Formation. Amphipathic helical structures are needed for apolipoprotein to form rHDL, in which the nonpolar faces of the amphipathic helices orient toward lipids, and the polar faces orient toward the aqueous phase. The combination of a hydrophobic styrene moiety and charged maleic acid moiety provides the amphiphilic nature of SMAaf. It is conceivable that differences in the hydrophilic/hydrophobic balance (such as the styrene to maleic acid ratio) might affect the formation of discoidal nanoparticles. As required for apolipoproteins, high hydrophobicity is also required for polymers to insert effectively among the lipids, but too much hydrophobicity inhibits solubilization, possibly because of self-association.[27] Furthermore, it is possible to insert polymers with small pendant groups into liposomal membranes regardless of the packing defects.[26] For such reasons, SMAaf with a styrene to maleic acid ratio of 2/1 might be more appropriate for efficient solubilization. Unlike apolipoproteins with variously charged side chains, common charged groups in synthetic polymers lead to conformational transitions from the extended to the globular state in keen response to the solution pH. Such characteristic behaviors are referred to as hypercoiling, and SMAaf is a representative example of hypercoiling polymers.[28] Poly(2-ethacrylic acid), another synthetic polymer classified as a hypercoiling polymer, has been shown to interact with phospholipids and form discoidal nanoparticles with reductions in pH.[29,30] Because the ethyl group is less hydrophobic than styrene, it is postulated that the hydrophobicity of the polymer is insufficient for formation of discoidal nanoparticles at neutral pH. Only when the solution pH decreases will the hydrophobicity increase because of partial protonation of the carboxy group and, thus, enable the polymer to disrupt the liposomal membrane. Poly(methacrylic acid), closely resembling but even less hydrophobic than poly(2-ethacrylic acid), might also have induced spontaneous turbidity clearance of DMPC vesicles under more acidic conditions. Further investigation may enable us to find more optimal polymer for the formation of discoidal nanoparticles applied as novel delivery vehicles.

4.3. Potential Applications of SMAaf as Therapeutic Agents for Cardiovascular Disease. Epidemiological studies have shown that HDL is protective against cardiovascular disease.[31] One of the protective functions of HDL arises from its central role in reverse cholesterol transport in which cellular lipid efflux mediated by apolipoprotein is the first step. The ability of apolipoprotein to solubilize phospholipid bilayers has been linked to the ability to promote cellular lipid efflux.[32] Thus, apoA-I and its mimetic peptides are currently being developed as therapeutic agents for cardiovascular disease. In fact, infusion of a genetic variant of apoA-I has been attempted to reduce cardiovascular risk.[33] Furthermore, rHDL contributes to cardioprotective effects partly by serving as an acceptor for cellular free cholesterol.[34] In this context, SMAaf and lipid–SMAaf complexes can be also developed as therapeutic agents for cardiovascular disease. However, because the composition of HDL determines its functional properties rather than the levels of circulating HDL, the effectiveness of these complexes, if any, should be assessed cautiously.

4.4. Perspectives on Bioimaging Applications of Lipid–SMAaf Complexes Relative to Those of Liposomes. Lipid–SMAaf complexes are considered to be superior to liposomes as delivery vehicles of drugs and/or imaging agents in some respects. For example, lipid–SMAaf complexes can be prepared with highly homogeneous size distribution only by mixing, without using a particular sizing procedure. In addition, colloidal properties of lipid–SMAaf complexes that are resistant to freeze-drying without a lyoprotectant are pharmaceutically attractive. Higher stability against lyophilization than that of liposomes may likely arise because of the absence of an internal aqueous phase.

DOI: 10.1021/acs.langmuir.5b03438
Langmuir 2015, 31, 12719–12726

Furthermore, surface modifications to avoid recognition as foreign particles may not be required for lipid−SMAaf complexes because of the nature of HDL-mimicking lipid particles.

Disruption of lipid−SMAaf complexes in a pH-sensitive manner also can be advantageous. For example, HDL-sized nanoparticles delivered to tumor acidic microenvironments (pH 6.0−7.0) can be enlarged and retained. Furthermore, considering the applications as drug carriers, pH-induced disruption of the particles may be useful for drug release from the platform at mildly acidic pH as observed within the intracellular environments, such as endosomes. In fact, SMA-loaded liposomes have been shown to be attractive, new pH-sensitive vehicles that allow cytoplasmic delivery of therapeutic agents.[35]

Discoidal rHDL composed of apoA-I has been exploited as an imaging probe of atherosclerosis by making use of the innate function of HDL to interact with macrophages.[36] SMAaf is biologically inert; consequently, SMAaf-based nanoparticles exert no particular functions utilized for cellular uptake, which perhaps contribute to reducing their nonspecific accumulation. Lipid−SMAaf complexes can be modified to target specific cells by attaching a ligand. Thus, lipid−SMAaf complexes might offer a promising alternative not only as platforms for membrane proteins but also as delivery vehicles. We are currently investigating the efficacy of the installed functionality and *in vivo* biodistribution of lipid−SMAaf complexes.

AUTHOR INFORMATION

Corresponding Author

*Tel +81-78-441-7540; Fax +81-78-441-7541; e-mail masatnk@kobepharma-u.ac.jp (M.T.).

Notes

The authors declare no competing financial interest.

ACKNOWLEDGMENTS

This work was supported in part by a JSPS KAKENHI Grant-in-Aid for Young Scientists (B) (No. 24790056), by the Platform Project for Supporting Drug Discovery and Life Science Research (Platform for Drug Discovery, Informatics, and Structural Life Science) from the Japan Agency for Medical Research and Development (AMED), and by The Uehara Memorial Foundation. The authors thank Enago for the English language review.

ABBREVIATIONS

apoA-I, apolipoprotein A-I; DLS, dynamic light scattering; DMPC, dimyristoylphosphatidylcholine; GP, generalized polarization; HDL, high-density lipoprotein; MSP, membrane scaffold protein; POPC, 1-palmitoyl-2-oleoylphosphatidylcholine; SMAaf, hydrolyzed acid form of styrene−maleic anhydride copolymer; TEM, transmission electron microscopy; rHDL, reconstituted HDL.

REFERENCES

(1) Phillips, M. C. New insights into the determination of HDL structure by apolipoproteins: Thematic review series: high density lipoprotein structure, function, and metabolism. *J. Lipid Res.* **2013**, *54* (8), 2034−48.

(2) Segrest, J. P.; Garber, D. W.; Brouillette, C. G.; Harvey, S. C.; Anantharamaiah, G. M. The amphipathic alpha helix: a multifunctional structural motif in plasma apolipoproteins. *Adv. Protein Chem.* **1994**, *45*, 303−69.

(3) Guha, M.; Gantz, D. L.; Gursky, O. Effects of acyl chain length, unsaturation, and pH on thermal stability of model discoidal HDLs. *J. Lipid Res.* **2008**, *49* (8), 1752−61.

(4) Chromy, B. A.; Arroyo, E.; Blanchette, C. D.; Bench, G.; Benner, H.; Cappuccio, J. A.; Coleman, M. A.; Henderson, P. T.; Hinz, A. K.; Kuhn, E. A.; Pesavento, J. B.; Segelke, B. W.; Sulchek, T. A.; Tarasow, T.; Walsworth, V. L.; Hoeprich, P. D. Different apolipoproteins impact nanolipoprotein particle formation. *J. Am. Chem. Soc.* **2007**, *129* (46), 14348−54.

(5) Nath, A.; Atkins, W. M.; Sligar, S. G. Applications of phospholipid bilayer nanodiscs in the study of membranes and membrane proteins. *Biochemistry* **2007**, *46* (8), 2059−69.

(6) Midtgaard, S. R.; Pedersen, M. C.; Kirkensgaard, J. J.; Sorensen, K. K.; Mortensen, K.; Jensen, K. J.; Arleth, L. Self-assembling peptides form nanodiscs that stabilize membrane proteins. *Soft Matter* **2014**, *10* (5), 738−52.

(7) Oda, M. N.; Hargreaves, P. L.; Beckstead, J. A.; Redmond, K. A.; van Antwerpen, R.; Ryan, R. O. Reconstituted high density lipoprotein enriched with the polyene antibiotic amphotericin B. *J. Lipid Res.* **2006**, *47* (2), 260−7.

(8) Ghosh, M.; Singh, A. T.; Xu, W.; Sulchek, T.; Gordon, L. I.; Ryan, R. O. Curcumin nanodisks: formulation and characterization. *Nanomedicine* **2011**, *7* (2), 162−7.

(9) Ryan, R. O. Nanobiotechnology applications of reconstituted high density lipoprotein. *J. Nanobiotechnol.* **2010**, *8*, 28.

(10) Orwick, M. C.; Judge, P. J.; Procek, J.; Lindholm, L.; Graziadei, A.; Engel, A.; Grobner, G.; Watts, A. Detergent-free formation and physicochemical characterization of nanosized lipid-polymer complexes: Lipodisq. *Angew. Chem., Int. Ed.* **2012**, *51* (19), 4653−7.

(11) Maeda, H.; Wu, J.; Sawa, T.; Matsumura, Y.; Hori, K. Tumor vascular permeability and the EPR effect in macromolecular therapeutics: a review. *J. Controlled Release* **2000**, *65* (1−2), 271−84.

(12) Donati, I.; Gamini, A.; Vetere, A.; Campa, C.; Paoletti, S. Synthesis, characterization, and preliminary biological study of glycoconjugates of poly(styrene-co-maleic acid). *Biomacromolecules* **2002**, *3* (4), 805−12.

(13) Li, T.; Zhou, C.; Jiang, M. UV absorption spectra of polystyrene. *Polym. Bull.* **1991**, *25* (2), 211−216.

(14) Kawaguchi, S.; Kitano, T.; Ito, K. Dissociation behavior of poly(fumaric acid) and poly(maleic acid). 3. Infrared and ultraviolet spectroscopy. *Macromolecules* **1992**, *25* (4), 1294−1299.

(15) Palgunachari, M. N.; Mishra, V. K.; Lund-Katz, S.; Phillips, M. C.; Adeyeye, S. O.; Alluri, S.; Anantharamaiah, G. M.; Segrest, J. P. Only the two end helixes of eight tandem amphipathic helical domains of human apo A-I have significant lipid affinity. Implications for HDL assembly. *Arterioscler., Thromb., Vasc. Biol.* **1996**, *16* (2), 328−38.

(16) Li, X.; Mooney, P.; Zheng, S.; Booth, C. R.; Braunfeld, M. B.; Gubbens, S.; Agard, D. A.; Cheng, Y. Electron counting and beam-induced motion correction enable near-atomic-resolution single-particle cryo-EM. *Nat. Methods* **2013**, *10* (6), 584−90.

(17) Parasassi, T.; De Stasio, G.; Ravagnan, G.; Rusch, R. M.; Gratton, E. Quantitation of lipid phases in phospholipid vesicles by the generalized polarization of Laurdan fluorescence. *Biophys. J.* **1991**, *60* (1), 179−89.

(18) Pownall, H. J.; Massey, J. B.; Kusserow, S. K.; Gotto, A. M., Jr. Kinetics of lipid–protein interactions: interaction of apolipoprotein A-I from human plasma high density lipoproteins with phosphatidylcholines. *Biochemistry* **1978**, *17* (7), 1183−8.

(19) Zhang, L.; Song, J.; Cavigiolio, G.; Ishida, B. Y.; Zhang, S.; Kane, J. P.; Weisgraber, K. H.; Oda, M. N.; Rye, K. A.; Pownall, H. J.; Ren, G. Morphology and structure of lipoproteins revealed by an optimized negative-staining protocol of electron microscopy. *J. Lipid Res.* **2011**, *52* (1), 175−84.

(20) Parasassi, T.; Conti, F.; Gratton, E. Time-resolved fluorescence emission spectra of Laurdan in phospholipid vesicles by multifrequency phase and modulation fluorometry. *Cell. Mol. Biol.* **1986**, *32* (1), 103−8.

DOI: 10.1021/acs.langmuir.5b03438
Langmuir 2015, 31, 12719−12726

(21) Shaw, A. W.; McLean, M. A.; Sligar, S. G. Phospholipid phase transitions in homogeneous nanometer scale bilayer discs. *FEBS Lett.* **2004**, *556* (1−3), 260−4.
(22) Galla, H. J.; Hartmann, W. Excimer-forming lipids in membrane research. *Chem. Phys. Lipids* **1980**, *27* (3), 199−219.
(23) Drummond, D. C.; Meyer, O.; Hong, K.; Kirpotin, D. B.; Papahadjopoulos, D. Optimizing liposomes for delivery of chemotherapeutic agents to solid tumors. *Pharmacol. Rev.* **1999**, *51* (4), 691−743.
(24) Zhang, R.; Sahu, I. D.; Liu, L.; Osatuke, A.; Comer, R. G.; Dabney-Smith, C.; Lorigan, G. A. Characterizing the structure of lipodisq nanoparticles for membrane protein spectroscopic studies. *Biochim. Biophys. Acta, Biomembr.* **2015**, *1848*, 329−33.
(25) Raussens, V.; Mah, M. K.; Kay, C. M.; Sykes, B. D.; Ryan, R. O. Structural characterization of a low density lipoprotein receptor-active apolipoprotein E peptide, ApoE3-(126−183). *J. Biol. Chem.* **2000**, *275* (49), 38329−36.
(26) Scheidelaar, S.; Koorengevel, M. C.; Pardo, J. D.; Meeldijk, J. D.; Breukink, E.; Killian, J. A. Molecular model for the solubilization of membranes into nanodisks by styrene maleic Acid copolymers. *Biophys. J.* **2015**, *108* (2), 279−90.
(27) Datta, G.; Chaddha, M.; Hama, S.; Navab, M.; Fogelman, A. M.; Garber, D. W.; Mishra, V. K.; Epand, R. M.; Epand, R. F.; Lund-Katz, S.; Phillips, M. C.; Segrest, J. P.; Anantharamaiah, G. M. Effects of increasing hydrophobicity on the physical-chemical and biological properties of a class A amphipathic helical peptide. *J. Lipid Res.* **2001**, *42* (7), 1096−104.
(28) Tonge, S. R.; Tighe, B. J. Responsive hydrophobically associating polymers: a review of structure and properties. *Adv. Drug Delivery Rev.* **2001**, *53* (1), 109−22.
(29) Thomas, J. L.; Devlin, B. P.; Tirrell, D. A. Kinetics of membrane micellization by the hydrophobic polyelectrolyte poly(2-ethylacrylic acid). *Biochim. Biophys. Acta, Biomembr.* **1996**, *1278* (1), 73−8.
(30) Borden, K. A.; Eum, K. M.; Langley, K. H.; Tan, J. S.; Tirrell, D. A.; Voycheck, C. L. pH-dependent vesicle-to-micelle transition in an aqueous mixture of dipalmitoylphosphatidylcholine and a hydrophobic polyelectrolyte. *Macromolecules* **1988**, *21* (8), 2649−2651.
(31) Gordon, T.; Castelli, W. P.; Hjortland, M. C.; Kannel, W. B.; Dawber, T. R. High density lipoprotein as a protective factor against coronary heart disease. The Framingham Study. *Am. J. Med.* **1977**, *62* (5), 707−14.
(32) Gillotte, K. L.; Zaiou, M.; Lund-Katz, S.; Anantharamaiah, G. M.; Holvoet, P.; Dhoest, A.; Palgunachari, M. N.; Segrest, J. P.; Weisgraber, K. H.; Rothblat, G. H.; Phillips, M. C. Apolipoprotein-mediated plasma membrane microsolubilization. Role of lipid affinity and membrane penetration in the efflux of cellular cholesterol and phospholipid. *J. Biol. Chem.* **1999**, *274* (4), 2021−8.
(33) Nissen, S. E.; Tsunoda, T.; Tuzcu, E. M.; Schoenhagen, P.; Cooper, C. J.; Yasin, M.; Eaton, G. M.; Lauer, M. A.; Sheldon, W. S.; Grines, C. L.; Halpern, S.; Crowe, T.; Blankenship, J. C.; Kerensky, R. Effect of recombinant ApoA-I Milano on coronary atherosclerosis in patients with acute coronary syndromes: a randomized controlled trial. *Jama* **2003**, *290* (17), 2292−300.
(34) Shaw, J. A.; Bobik, A.; Murphy, A.; Kanellakis, P.; Blombery, P.; Mukhamedova, N.; Woollard, K.; Lyon, S.; Sviridov, D.; Dart, A. M. Infusion of reconstituted high-density lipoprotein leads to acute changes in human atherosclerotic plaque. *Circ. Res.* **2008**, *103* (10), 1084−91.
(35) Banerjee, S.; Sen, K.; Pal, T. K.; Guha, S. K. Poly(styrene-co-maleic acid)-based pH-sensitive liposomes mediate cytosolic delivery of drugs for enhanced cancer chemotherapy. *Int. J. Pharm.* **2012**, *436* (1−2), 786−97.
(36) Frias, J. C.; Ma, Y.; Williams, K. J.; Fayad, Z. A.; Fisher, E. A. Properties of a versatile nanoparticle platform contrast agent to image and characterize atherosclerotic plaques by magnetic resonance imaging. *Nano Lett.* **2006**, *6* (10), 2220−4.

DOI: 10.1021/acs.langmuir.5b03438
Langmuir 2015, 31, 12719−12726